Rigorous Generation of Digital Orthophotos from SPOT Images

Abstract

An original method that rigorously generates digital orthophotos from SPOT images is presented. In place of the ray tracing method, we have developed an algorithm that determines the corresponding image coordinates for a ground element, provided that the time dependent orientation parameters and a DTM are available. In this paper, a rigorous bundle adjustment program for pushbroom scanning images that models the dynamic orientation for SPOT data is first developed. Incorporating the DTM, a non-linear equation is formulated that determines the image coordinates in the flight direction in terms of the sampling time for a ground element. The Newton-Raphson method is then applied in order to solve the non-linear equation. The along-track and across-track image coordinates for the corresponding ground element can thus be calculated. After a bilinear interpolation, the pixel grey value for the ground element in the orthophoto is determined. Experimental results indicate that the generated orthoimages attain an accuracy better than two-thirds of a pixel.

Introduction

The generation of orthophotos from remotely sensed images, such as aerial photographs, satellite images, and airborne scanning images, is an important task for various remote sensing applications. Employing this geometrical rectification, the image can be correctly georeferenced. The orthophotos may be generated using either the analog or the digital approach. It is not the purpose of this paper to discuss the analog approach. We will, instead, discuss the digital approach and propose an original and rigorous method for SPOT satellite data processing.

The digital rectification required to generate an orthoimage from an image may be accomplished in two ways. The first is the Anchorpoints method (Mayr and Heipke, 1988). In this method, a set of ground control points (GCPs) (i.e., the anchorpoints), are collected at locations which can be identified on both the image and on a corresponding map. Once enough GCP samples have been collected, the image coordinates are modeled as functions of the map coordinates using the least-squares method to fit low-order polynomials to the data (Jensen, 1986). For each pixel on the orthoimage, which has the same coordinate system as the map, the grey value is determined by locating the corresponding image position on the raw image followed by resampling. The method may be performed globally or locally. In the global approach, the transformation coefficients for the polynomials are kept throughout the whole image. On the other hand, the local approach subdivides the whole area into a number of Delaunay triangles (Devereux *et al.*, 1990; De Floriani *et al.*, 1989), with the vertices of each triangle used as the GCPs. The advantage of this method is that it is computationally fast (Mayr and Heipke, 1988). However, high frequency image distortions due to terrain relief can be rigorously compensated for only when extremely dense GCPs are available.

The second approach is the rigorous solution and is called the Pixel-by-Pixel approach (Mayr and Heipke, 1988). This approach considers the three-dimensional (3D) ground surface variations. Specifically, the associated DTM is utilized in the orthoimage generation. The correspondence between an image pixel and the conjugate ground element is characterized by the collinearity condition for central perspective images. In principle, there are two ways to do this. The first method, which is called the Direct or the Top-Down method, starts from the image space and projects each image pixel onto the object surface (Mayr and Heipke, 1988). This method is also known as the Ray-Tracing method (O'Neill and Dowman,1988). Conversely, it is possible to do the opposite, i.e., the Indirect or the Bottom-Up method (Mayr and Heipke, 1988; Wiesel, 1985). Starting from the object space, each ground element is projected onto the image space. The grey value of a ground element on the orthoimage is then resampled using the projected location and its neighboring pixel values on the raw image.

Despite many advantages of the Indirect method as compared to the Direct method (Mayr and Heipke, 1988; Wiesel, 1985), the Indirect method can be applied only to those situations when the transformation between the image space and the object space is reversible (Houssay and Brossier, 1988). For aerial photographs, for example, having a "point" as the perspective center, the transformation is explicitly reversible when the collinearity condition is applied. For SPOT images, on the other hand, the reversibility from 3D ground coordinates to 2D image coordinates for each point is hidden. As this implicit reversibility is not solved, currently the Direct method is used to generate orthoimages from SPOT data (O'Neill and Dowman, 1988).

After exploring the hidden reversibility, we will propose an Indirect method in this paper that determines the corresponding image point on a SPOT scene for a ground element when the 3D location of the ground element is given. Incorporating a DTM, a SPOT 1A image, and the orientation parameters, a non-linear equation is formulated to determine the along-track image coordinates in terms of the sampling time for a ground element. The Newton-Raphson method (Dyck *et at.*, 1982) is then applied to solve the non-linear equation. The across-track image coordinate can then be calculated ac-

Photogrammetric Engineering & Remote Sensing, Vol. 59, No. 5, May 1993, pp. 655–661.

0099-1112/93/5905–655$03.00/0

Liang-Chien Chen
Center for Space and Remote Sensing Research and Department of Civil Engineering, National Central University, Chung-Li, Taiwan 320, Republic of China

Liang-Hwei Lee
Department for Surveying and Mapping Engineering, Chung-Cheng Institute of Technology, Ta-Hsi, Taiwan 335, Republic of China

cording to the collinearity condition. After a bilinear interpolation, the pixel grey value for the ground element on the orthoimage is resampled.

Orientation Modeling

The sampling geometry for SPOT images is illustrated in Figure 1, where F.D. is the flight direction, f is the focal length, and PP_{tn} is the principal point at sampling time t_n. Due to its pushbroom scanning characteristics, a central perspective projection is maintained across track. On the other hand, a near parallel projection is maintained along the flight direction. For ground point "A" on a line sampled at time t_n, the corresponding image point "a" should satisfy the collinearity condition when the time dependent orientation parameters, i.e., (X^c, Y^c, Z^c, ω, ϕ, κ) at t_n, are applied. Similarly, for point "B" on the ground, its image point "b" follows the same condition when the different orientation parameters at time t_m are applied. The relationship among sampling lines is characterized by the dynamic orientation parameters which are modeled with low order polynomials as a function of the sampling time (Chen and Lee, 1990).

For a SPOT 1A panchromatic image, a full scene is composed of 6,000 by 6,000 pixels. The CCD size for each pixel is 13 by 13 μm. The nominal focal length 1.082 m. The sampling time interval between two consecutive lines is 0.0015 seconds. This 0.0015-second sampling interval may not be exactly the same during the SPOT sampling. In addition, the actual CCD size and focal length may differ from their nominal dimensions. Accordingly, deviations of those interior orientation related parameters will need to be compensated for by the scale affinity and the exterior orientation parameters as discussed later. The image coordinates in this paper are defined as

$$\begin{aligned} x_i &= 0, \\ y_i &= [\text{Pixel No.} - (6{,}000 + 1)/2] * 0.013 \text{ mm, and} \\ f &= 1082 \text{ mm}, \end{aligned} \quad (1)$$

where

x_i is the image coordinate along track for point i,
y_i is the image coordinate across track for point i, and
f is the focal length.

The collinearity equations (Slama, 1980) for central projective images are then modified to satisfy the SPOT sampling geometry: i.e.,

$$x_i = -f\frac{m_{11t}(X_i - X_t^c) + m_{12t}(Y_i - Y_t^c) + m_{13t}(Z_i - Z_t^c)}{m_{31t}(X_i - X_t^c) + m_{32t}(Y_i - Y_t^c) + m_{33t}(Z_i - Z_t^c)} \quad (2a)$$

$$S_i \cdot y_i = -f\frac{m_{21t}(X_i - X_t^c) + m_{22t}(Y_i - Y_t^c) + m_{23t}(Z_i - Z_t^c)}{m_{31t}(X_i - X_t^c) + m_{32t}(Y_i - Y_t^c) + m_{33t}(Z_i - Z_t^c)} \quad (2b)$$

where

X_i, Y_i, Z_i are the ground coordinates of point i;
m_{11t}, ..., m_{33t} are the elements of the rotation matrix expressed as functions of ω_t, φ_t, and κ_t;
X_t^c, Y_t^c, Z_t^c are the orbital parameters at time t;
ω_t, φ_t, κ_t are the attitude parameters at time t; and
S_y is the scale affinity.

The orbital and attitude parameters are characterized by second-order polynomials as functions of the sampling time t relative to the first scan line: i.e.,

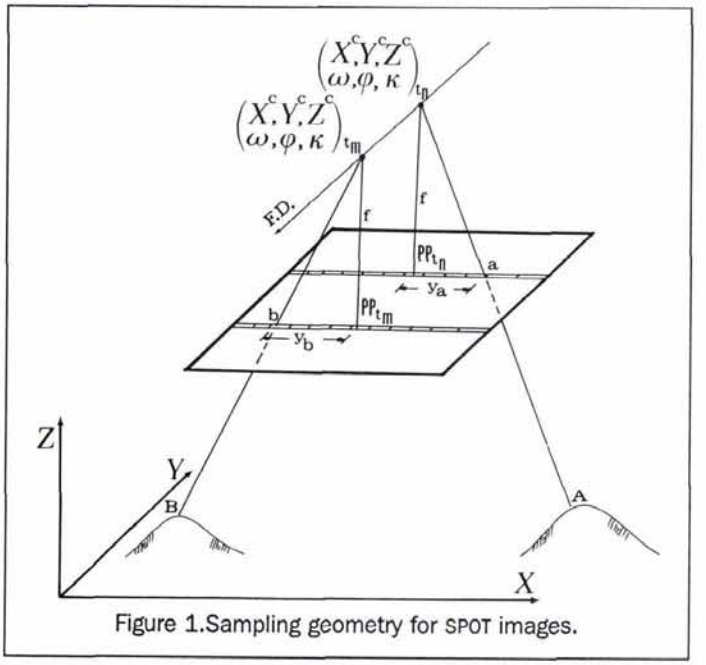

Figure 1. Sampling geometry for SPOT images.

$$\begin{aligned} X_t^c &= X_0 + X_1 t + X_2 t^2 \\ Y_t^c &= Y_0 + Y_1 t + Y_2 t^2 \\ Z_t^c &= Z_0 + Z_1 t + Z_2 t^2 \\ \omega_t &= \omega_0 + \omega_1 t + \omega_2 t^2 \\ \phi_t &= \phi_0 + \phi_1 t + \phi_2 t^2 \\ \kappa_t &= \kappa_0 + \kappa_1 t + \kappa_2 t^2 \end{aligned} \quad (3)$$

Through a least-squares adjustment for the photogrammetric problem, the orientation parameters are determined (Lee and Chen, 1988).

Rigorous Generation of Orthoimages from SPOT Data

We shall discuss first the algorithmic aspects of the Ray-Tracing method, which is currently used by many researchers for SPOT data processing (O'Neill and Dowman, 1988) and digitized aerial photographs (Mayr and Heipke, 1988; Wiesel, 1985; Houssay and Brossier, 1988). The details of the proposed Indirect method are then given.

Ray-Tracing Method

The Ray-Tracing method is illustrated in Figure 2a. Assuming that the orientation parameters, the DTM, and the coordinates of point P on the image plane, IP, are given. The tracing ray OP emerging from projection center O is then defined. The major task of orthographic generation is to determine the corresponding ground point I for image point P. The iterative procedure that determines the intersection point between the ray OP and the ground surface is stated as follows:

(1) Given an initial surface elevation Z_A, determine the planimetric coordinates of intersection point A between OP and the initial surface by employing Equations 2a and 2b.
(2) Trace surface point B, having the same planimetric position as A, i.e., $X_B = X_A$ and $Y_B = Y_A$, from the DTM to determine Z_B.
(3) Update the reference surface from $Z = Z_A$ to $Z = Z_B$, then repeat steps (1) and (2) to determine points C, D, E, F, G, H, and I until convergence.
(4) The ground point I corresponding to image point P is thus determined.

When the point correspondence is accomplished throughout

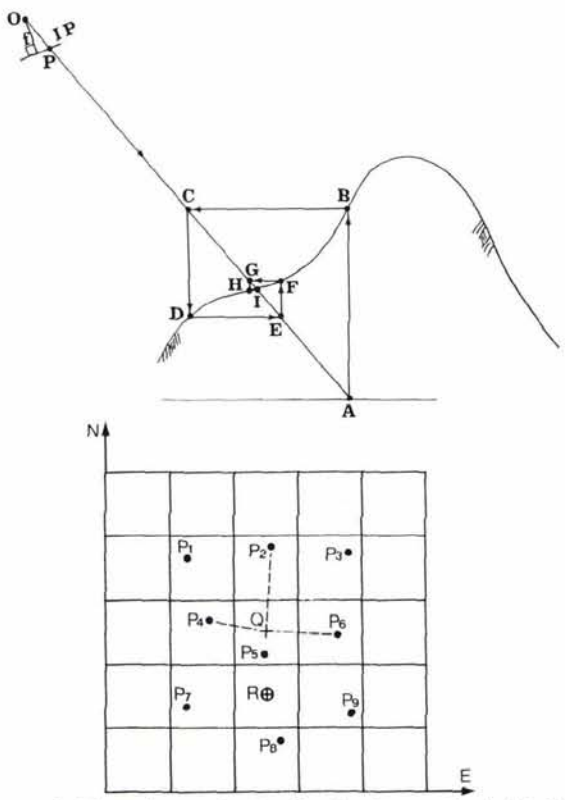

Figure 2. The scheme for the Ray Tracing method. (a) the tracing sequence. (b) pixel value resampling.

the entire image, the output image may be generated through a resampling procedure. Referring to Figure 2b, P_1, P_2, ..., to P_9 are the projected locations for the nine corresponding points. They are not spaced quite equally on the generated orthoimage, which has a map coordinate system. For pixel Q on the orthoimage, as shown in the figure, the grey value may be interpolated from its four closest neighboring points P_2, P_4, P_5, and P_6 using bilinear interpolation (Jensen, 1986).

The major advantage of the Ray Tracing method is that it can be applied to various remotely sensed images such as digitized aerial photographs, SPOT images, Landsat images, and airborne multispectral images. However, there are three obvious disadvantages:

- The iterative calculation for the intersecting point of the tracing ray and the ground surface may cause the computation to be heavy, especially when the surface normal vector has a direction similar to the tracing ray.
- In grey value resampling, the nearest neighboring points for an interpolating pixel need to be searched for in the real number field. Thus, the computation is rather intensive.
- The grey value is incorrect for those output pixels when no input pixel is directly mapped on. For instance, for a pixel R on the output image, as shown in Figure 2b, the grey value is not quite correct (Rosenfeld and Kak, 1982).

Accordingly, the direct method is limited in its computational efficiency and output image quality. On the contrary, the indirect method gives a better solution as far as SPOT images are concerned. The problem that the indirect method encounters is how to explore the hidden object-to-image reversibility. This will be discussed next.

The Proposed Indirect Method

Once the orientation parameters are determined and a DTM is given, the corresponding image position for a ground point may be determined by the following procedure:

(1) Orthographic projection from a SPOT image is a matter of selecting the suitable grey value for each output pixel from the raw image. Thus, the projected position on the raw image for an output pixel must be searched for in advance. The ground coordinates used in this investigation are in the Local Cartesian System to alleviate the influence of Earth curvature. However, the ground coordinate system in Taiwan is defined by the Transverse Mercator Projection. Accordingly, the coordinate system in this investigation is transformed to the Geographic Coordinate System first, then to the Geocentric Coordinate System, and finally to the Local Cartesian System (Lee, 1991). Referring to Figure 3, the ground coordinates (X, Y, Z) for ground point A are known. The location of the point on the orthoimage is A' and the corresponding point on the raw image is "a." The first step in our method is to determine the line number of "a," i.e., the coordinate along the flight direction, F.D. Then the sample number, i.e., the across-track coordinate, is calculated. The determination of the line number is equivalent to determining the sampling time for point "a."

Substituting $x_i = 0$ in Equation 1 into Equation 2a, we obtain

$$0 = -f\frac{m_{11t}(X_i - X_t^c) + m_{12t}(Y_i - Y_t^c) + m_{13t}(Z_i - Z_t^c)}{m_{31t}(X_i - X_t^c) + m_{32t}(Y_i - Y_t^c) + m_{33t}(Z_i - Z_t^c)}$$

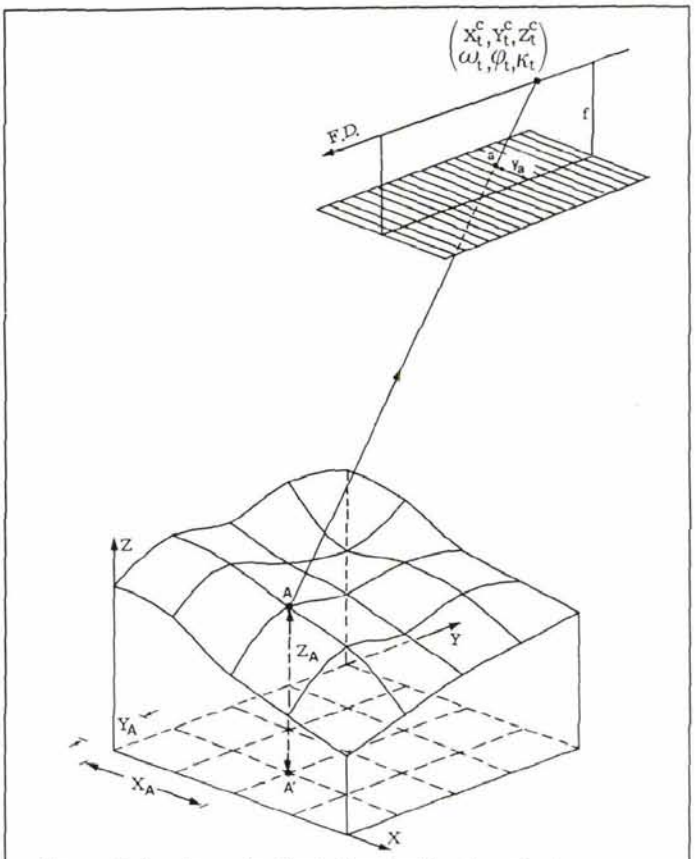

Figure 3. A schematic illustration for the described method.

Thus, the time dependent function $f(t_n)$ of the numerator,

$$f(t_n) = m_{11t}(X_i - X_f^c) + m_{12t}(Y_i - Y_f^c) + m_{13t}(Z_i - Z_f^c) = 0 \quad (4)$$

is valid.

(2) We apply the Newton-Raphson method (Dyck *et al.*, 1982) in order to solve the non-linear Equation 4 when determining the sampling time t_a of "a" for the ground point A, in which the ground coordinates X_A, Y_A, and Z_A are introduced from the DTM. The iteration is expressed as

$$t_{n+1} = t_n - \frac{f(t_n)}{f'(t_n)} = t_n - \frac{f(t_n)}{|f(t_n) - f(t_{n-1})|/(t_n - t_{n-1})} \quad (5)$$

where $n = 0, 1, 2, \ldots$, until

$|t_{n+1} - t_n| < 10^{-6}$ is satisfied.

(3) When the sampling time t_a is calculated, the along-track image coordinate of "a" is

$$(\text{Line No.})_a = t_a / 0.0015. \quad (6)$$

(4) Substituting t_a into Equation 2b, we may determine the across-track image coordinate in a pixel as

$$(\text{Sample No.})_a = y_a / 0.013 \text{ mm}. \quad (7)$$

After determining the corresponding point coordinates (line, sample) for a ground element on the raw image, the grey value on the output orthoimage is calculated using bilinear interpolation based on its four nearest neighboring points. The search for the four nearest neighboring points for a point with coordinates (x, y) is performed by simply selecting the four integer pixels in the $(x - 1, x + 1)$ and $(y - 1, y + 1)$ range. As there is no need to search for the nearest neighboring points in the real number field, as in the direct method, this method is more efficient and less biased.

Experimental Results

The experiment includes tests of the proposed method for orthoimage generation from a SPOT 1A panchromatic image. The image was sampled on 15 January 1987 with a 10.4° incidence angle and covers an area of central west Taiwan. Three cases are studied. In the first case, an orthoimage of 550 by 500 pixels, i.e., the same size as four 1:5,000-scale photo basemap sheets and with 160 m of terrain relief, is generated and investigated. In the second case, an orthoimage covering an area of 550 by 500 pixels with 540 m of terrain relief is studied. In the third case, 24 ground check points distributed around the entire SPOT scene are selected to verify the model fidelity.

The object coordinates for the ground control points (GCPs) and check points (CKPs) are digitized from 1:5,000-scale photo base maps in three test cases. The maps and the DTMs with a 40- by 40-mm grid size were acquired from the Geographic Data Base of Taiwan (Fu, 1987). The contour lines on the maps and the DTMs were stereoscopically generated from 1:15,000-scale aerial photographs using Zeiss Planicomp C-100 analytical plotters. Based on the accuracy specifications of the Geographic Data Base, the horizontal tolerance for 90 percent of all well defined planimetric features is 0.3 mm on the map. This is equivalent to an error of 1.5 m on the ground. The digitizing error is estimated to be 0.15 mm on the map. Thus, the total error for GCPs and CKPs is about 1.67 m on the ground with a 90 percent confidence interval. This error with a 90 percent confidence interval, 1.645σ, is equivalent to about 1 m standard error. On the vertical aspect, 90 percent of elevations interpolated from the maps are correct within one-half the contour interval. The contour interval in the test areas of this investigation is 10 m. Thus, the vertical tolerance for 90 percent of elevations is within 5 m. The accuracy tolerance for 90 percent of elevations of the DTMs is also 5 m. Those elevation errors could introduce a planimetric error which is less than 0.1 pixels in the orthoimage generation when a SPOT scene having a 10.4° incidence angle is used (Lee, 1991).

The orientation parameters were determined using a bundle adjustment (Lee and Chen, 1988) in which second-order polynomials were used to model the dynamic orientation parameters with respect to sampling times. The full scene, consisting of the test image and the 21 GCPs marked with squares, is shown in Figure 4. In the figure, the 24 triangular marks are the check points for the Case III evaluation. The calculated exterior orientation parameters are listed in Table 1. The vectors of the image residuals after bundle adjustment for the 21 GCPs are shown in Figure 5. The analysis for the image residuals is briefly listed in Table 2 in which the RMS of the residuals is 0.19 pixels along track and 0.18 pixels across track.

Case I

A subscene of 600 by 600 pixels is cut from the raw image, as indicated in Figure 6, to study orthoimage generation in an area of rolling terrain. The test site is located at Houlong where the longitude and latitude of the site center are 120°46′ and 24°36′, respectively. The elevation ranges from 10 m to 170 m. The DTM is resampled from a 40m by 40m grid to a 10m by 10m grid using cubic convolution. Using the DTM, the determined orientation parameters, and the subscene, the generated orthoimage of 550 by 500 pixels is shown in Figure 7. Twenty-five check points are marked in the figure. The error vectors for the check points are plotted in Figure 8. The error is briefly analyzed in Table 3, in which the RMSE is 5.7 m for the X coordinate and 5.4 m for the Y coordinate. The computation time for generating the orthoimage is 11 minutes on a VAX 3900 work station. The work station is a 3.8 MIP machine.

TABLE 1. CALCULATED EXTERIOR ORIENTATION PARAMETERS

X_0	Y_0	Z_0	ω_0	ψ_0	κ_0
X_1	Y_1	Z_1	ω_1	ψ_1	κ_1
X_2	Y_2	Z_2	ω_2	ψ_2	κ_2
−35164.57	−262740.38	827883.83	10.399883	−2.016735	−10.162549
6504.06	−1577.94	−83.48	−0.000248	−0.000291	−0.000291
−6.98	−1.227	−0.52	0.000034	0.000046	0.000039
	X_0, Y_0, Z_0 : m X_1, Y_1, Z_1 : m/sec X_2, Y_2, Z_2 : m/sec²			$\omega_0, \psi_0, \kappa_0$: deg $\omega_1, \psi_1, \kappa_1$: deg/sec $\omega_2, \psi_2, \kappa_2$: deg/sec²	

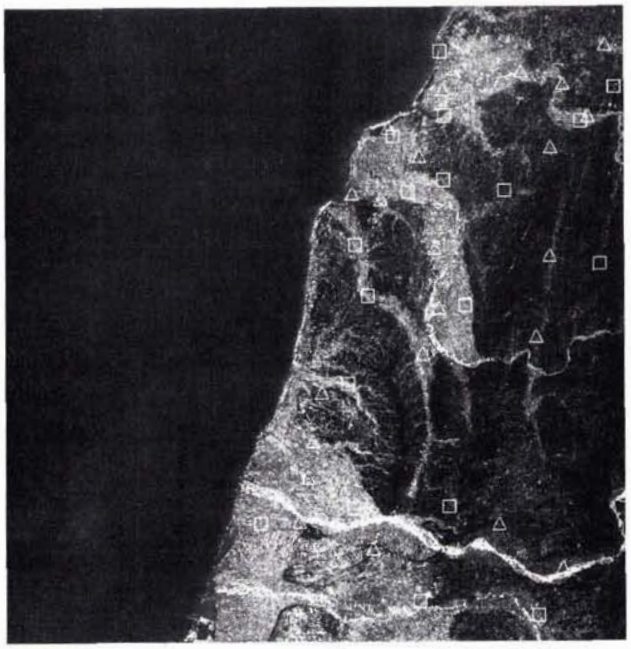

Figure 4. The test SPOT image. Squares are ground control points (GCPs). Triangles are check points (CKPs) in Case III. (© SPOT Image, copyright 1987 CNES.)

TABLE 2. IMAGE RESIDUALS FOR GROUND CONTROL POINTS (GCPS)

	Max. (pixel)	Min. (pixel)	RMS (pixel)
x	0.31	−0.32	0.19
y	0.22	−0.46	0.18

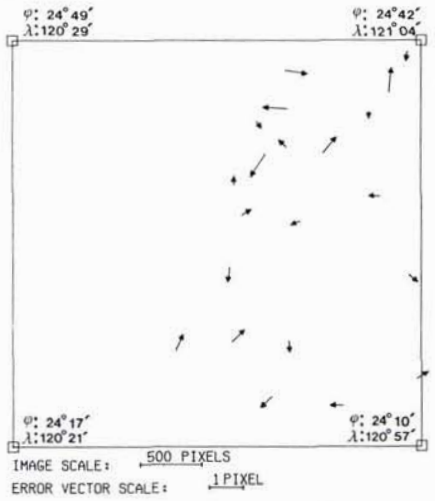

Figure 5. Residual ground control point (GCP) vectors.

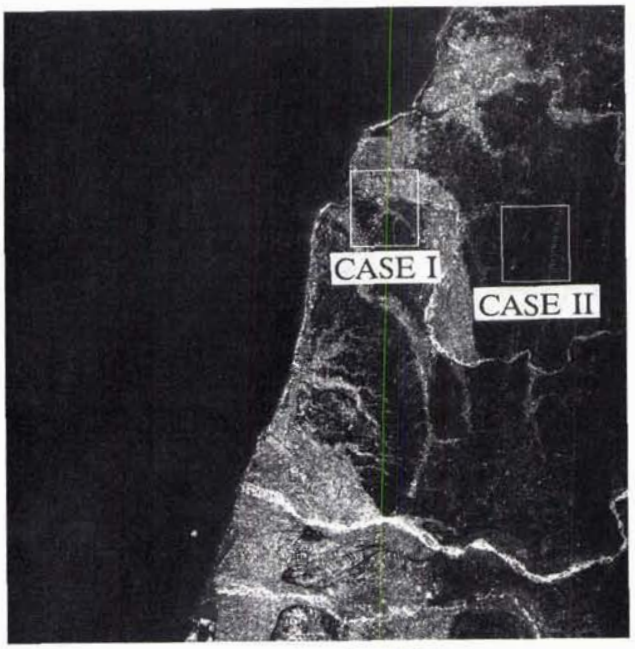

Figure 6. The test sites for Case I and Case II. (© SPOT Image, 1987 CNES.)

TABLE 3. ACCURACY ANALYSIS FOR CASE I

	Max. (m)	Min. (m)	RMSE (m)
X	10.6	−10.3	5.7
Y	11.1	−9.2	5.4

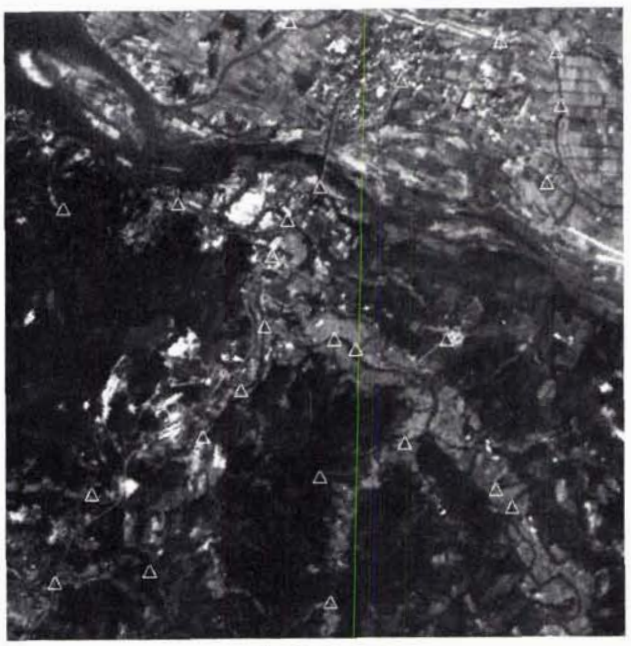

Figure 7. The generated orthoimage and check points for Case I.

Case II

The second subscene of 600 by 600 pixels is also cut from the same SPOT image as illustrated in Figure 6 in order to in-

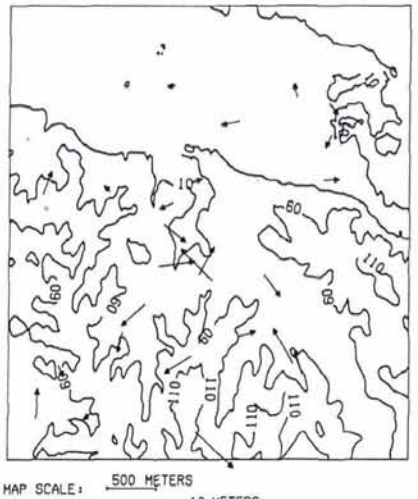

Figure 8. The error vectors for Case I.

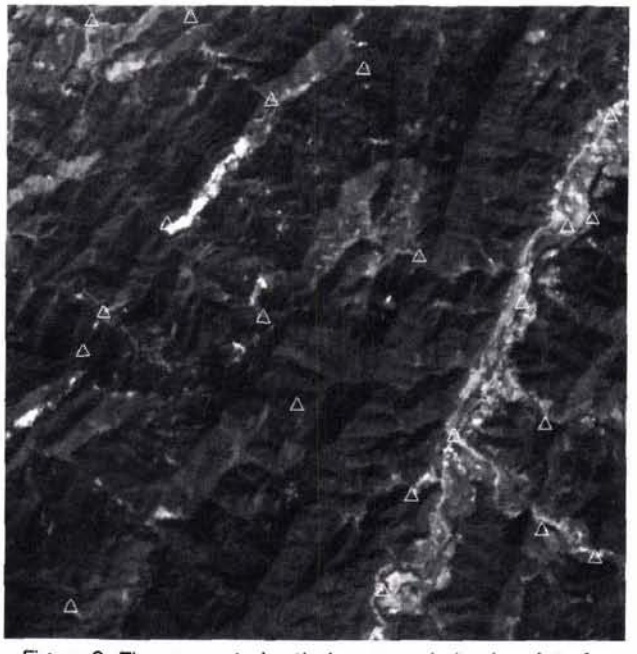

Figure 9. The generated orthoimage and check points for Case II.

vestigate the proposed method on a rugged terrain area. The test site is located at Hsitang where the longitude and latitude of the site center are 120°54′ and 24°33′, respectively. The terrain varies from 50 m to 590 m in elevation. The same method is reapplied. The generated orthoimage of 550 by 500 pixels is shown in Figure 9. The 22 check points are also marked. The error vectors for the check points are shown in Figure 10. The error is briefly analyzed in Table 4, in which the RMSE is 6.5 m for the X coordinate and 6.6 m for the Y coordinate. The computation time is the same as in *Case I*.

TABLE 4. ACCURACY ANALYSIS FOR CASE II

	Max. (m)	Min. (m)	RMSE (m)
X	11.3	−11.8	6.5
Y	11.4	−12.9	6.6

Case III

To verify model fidelity for the whole scene, we selected 24 ground check points spread throughout the entire SPOT image, instead of physically generating an orthoimage. This means that the 3D ground coordinates of the check points are used to calculate corresponding locations on the raw image, as compared to image coordinates being measured manually. The locations of the check points are marked with triangles as shown in Figure 3. The elevation range for the CKPs is 950 m. The error vectors are shown in Figure 11. The error is briefly analyzed in Table 5, in which the RMSE is 0.61 pixels along the flight direction and is 0.45 pixels across track.

A summary of the experimental results is as follows:

- The RMS of the image residuals for the control points after bundle adjustment is (0.19 pixels, 0.18 pixels).
- The RMSE of the generated orthoimage reaches (5.7 m, 5.4 m) for rolling terrain.
- For rugged terrain, the RMSE of the generated orthoimage reaches (6.5 m, 6.6 m).
- For evaluation of model fidelity for the entire scene with 950 m of terrain relief, the RMSE is (0.61 pixels, 0.45 pixels).
- Examining the results, it is found that the accuracy in all three cases is better than two-thirds of a pixel for the image scale.
- It has been discussed that among the several methods for orthoimage generation from SPOT data, the Top-Down method and the proposed Bottom-Up method are the most rigorous. Because those two methods satisfy the collinearity condition, they have the same theoretical basis. The only difference is in the opposite tracing directions. This difference causes different computational loads. According to the report by O'Neill and Dowman (1988), 60 minutes was spent to generate an orthoimage with 512 by 512 pixels from a SPOT subscene using the Top-Down method on a Sun 3 work station. The work station is a 3 MIP machine. We, on the other hand, spent 11 minutes to generate an orthoimage with 550 by 500 pixels on a 3.8 MIP VAX 3900 machine. It could be estimated that the computational load of the proposed method is about one-fourth of the Top-Down method.
- The DTMs used in Case I and Case II delineate the terrain height. Thus, if a DTM which delineates the canopy height is utilized, a higher accuracy is theoretically expected.

Conclusions

An indirect method for generating orthoimages from SPOT digital images is given. In contrast to the direct method, we explore the hidden reversibility from object space to image space. The theory is rigorous. The experimental results also demonstrate that the accuracy is better than two-thirds of a pixel. The test area covers both rolling and rugged terrain. The entire scene is also investigated for global fidelity. The proposed method is easy to implement. Accordingly, we may consider the method as applicable to other cases. It is also demonstrated that the proposed methods is superior to the Top-Down method as far as the computational load is concerned.

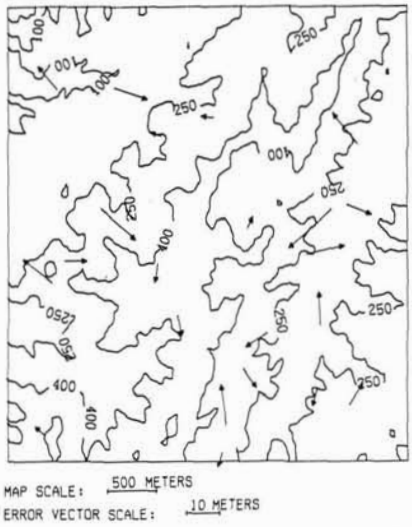

Figure 10. The error vectors for Case II.

TABLE 5. ACCURACY ANALYSIS FOR CASE III

	Max. (pixel)	Min. (pixel)	RMSE (pixel)
x	1.50	−0.69	0.61
y	1.04	−0.47	0.45

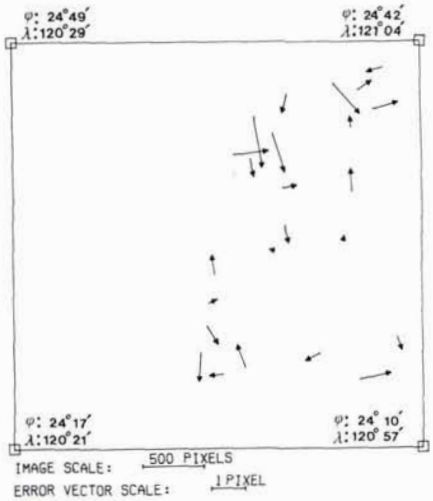

Figure 11. The error vectors for Case III.

Acknowledgment

This investigation was supported by the Remote Sensing Branch of the Council of Agriculture under Project Nos. 1989-01F and 1990-01K. The authors wish to thank their co-workers in the Center for Space and Remote Sensing Research at the National Central University for their valuable contribution to this paper. Specifically, we acknowledge the assistance of Jiann-Yeou Rau and Chih-Shiue Yan.

References

Chen, L.-C., and L.-H. Lee, 1990. A Systematic Approach to Digital Mapping Using SPOT Satellite Imagery. *Transactions of the Chinese Institute of Engineers*, Series D, 2(1):53–62.

De Floriani, L., B. Falcidieno, and C. Pienovi, 1985. Delaunay-Based Representation of Surfaces Defined Over Arbitrary Shaped Domains, *Computer Vision, Graphics, and Image Processing*, 32(1):127–140.

Devereux, B. J., R. M. Fuller, L. Carter, and R. J. Parsell, 1990. Geometric Correction of Airborne Scanner Imagery by Matching Delaunay Triangles, *International Journal of Remote Sensing*, 11(12):2237–2251.

Dyck, V. A., J. A. Lawson, J. D. Smith, and R. J. Beach, 1982. *Computing—An Introduction to Structural Problem Solving Using PASCAL*, Reston Publishing Company, Reston, Virginia, 625 p.

Fu, A.-M., 1987. The Establishment of the Base Map System and Its Applications, *The Journal of Chinese Society of Photogrammetry and Remote Sensing*, (12):1–64 (in Chinese).

Houssay, P., and R. Brossier, 1988. Digital Orthophotograph at IGN—France, *International Archives of Photogrammetry and Remote Sensing*, Kyoto, Japan, 27(B10):IV346–IV352.

Jensen, R. J., 1986. *Introductory Digital Image Processing*, Prentice-Hall, Englewood Cliffs, New Jersey, 379 p.

Lee, L.-H., 1991. *A Computational Vision Approach to Geometrical Analysis for SPOT Images*. Ph. D. Dissertation, National Central University, Chung-Li, Taiwan, 273 p. (in Chinese).

Lee, L.-H., and L.-C. Chen, 1988. Bundle Adjustment with Additional Parameters for SPOT Stereopairs, International Archives of Photogrammetry and Remote Sensing, Kyoto, Japan, 27(B8):III1–III10.

Mayr, W., and C. Heipke, 1988. A Contribution to Digital Orthophoto Generation, *International Archives of Photogrammetry and Remote Sensing*, Kyoto, Japan, 27(B11):IV430–IV439.

O'Neill, M. A., and I. J. Dowman, 1988. The Generation of Epipolar Synthetic Stereo Mates for SPOT Images Using a DEM, *International Archives of Photogrammetry and Remote Sensing*, Kyoto, Japan, 27(B3):587–598.

Rosenfeld, A., and A. Kak, 1982. *Digital Picture Processing*, Vol. 2, Second Edition, Academic Press, New York, New York, 349 p.

Slama, C. C (editor), 1980. *Manual of Photogrammetry*, Fourth Edition, Society of Photogrammetry, Falls Church, Virginia, 1056 p.

Wiesel, J. W., 1985. Digital Image Processing for Orthophoto Generation, *Photogrammetria*, 40(2):69-76.

(Received 27 December 1991; revised and accepted 3 November 1992)